

# EUROPHYSICS LETTERS

OFFPRINT

Vol. 73 • Number 6 • pp. 820–825

## Fluctuation-induced pattern formation in a surface reaction

\*\*\*

J. STARKE, C. REICHERT, M. EISWIRTH, H. H. ROTERMUND and G. ERTL



Published under the scientific responsibility of the

## EUROPEAN PHYSICAL SOCIETY

Incorporating

JOURNAL DE PHYSIQUE LETTRES • LETTERE AL NUOVO CIMENTO



## Fluctuation-induced pattern formation in a surface reaction

J. STARKE<sup>1</sup>, C. REICHERT<sup>1</sup>, M. EISWIRTH<sup>2</sup>, H. H. ROTERMUND<sup>2</sup> and G. ERTL<sup>2</sup>

<sup>1</sup> *Interdisziplinäres Zentrum für Wissenschaftliches Rechnen und  
Institut für Angewandte Mathematik, Universität Heidelberg  
Im Neuenheimer Feld 294, D-69120 Heidelberg, Germany*

<sup>2</sup> *Fritz-Haber-Institut der Max-Planck-Gesellschaft  
Faradayweg 4-6, D-14195 Berlin, Germany*

received 11 November 2005; accepted in final form 31 January 2006

published online 17 February 2006

PACS. 05.40.-a – Fluctuation phenomena, random processes, noise, and Brownian motion.

PACS. 82.40.Np – Temporal and spatial patterns in surface reactions.

PACS. 89.75.-k – Complex systems.

**Abstract.** – Spontaneous nucleation, pulse formation and propagation failure have been observed experimentally in CO oxidation on Pt(110) at intermediate pressures ( $\approx 10^{-2}$  mbar). This phenomenon can be reproduced with a stochastic model that includes temperature effects. Nucleation occurs randomly due to fluctuations in the reaction processes, whereas the subsequent damping out essentially follows the deterministic path. Conditions for the occurrence of stochastic effects in the pattern formation during CO oxidation on Pt are discussed.

CO oxidation on platinum is probably the most extensively studied reaction in surface science. It exhibits nonlinear phenomena like phase transitions, oscillations and spatiotemporal pattern formation and serves as standard example for a system far from thermodynamic equilibrium in physics and chemistry [1]. The elementary steps of CO oxidation on platinum single-crystal surfaces at low ( $\lesssim 10^{-4}$  mbar) to intermediate pressures are well established: The reaction proceeds via a Langmuir-Hinshelwood mechanism with asymmetric inhibition of adsorption (preadsorbed CO blocks oxygen adsorption, but not vice versa) [2,3]. In addition, Pt(110) and Pt(100) (the surfaces corresponding to crystal planes with Miller indices (110) and (100), respectively) exhibit surface structural changes which play a crucial role for the reaction dynamics.

While on very small scales fluctuations in the reaction processes certainly do have an important influence even at low pressure in the gas phase ( $\approx 10^{-4}$  mbar), as was demonstrated in experiments with a field emitter tip and corresponding Monte Carlo simulations [4, 5], pattern formation on comparatively large surfaces ( $\approx 1$  cm<sup>2</sup>) could, in the same pressure range, successfully be modelled with (deterministic) partial differential equations for the surface coverages (reaction-diffusion equations), neglecting any temperature variations [2, 3]. The reason is that at low pressures each adsorbed CO molecule changes its site up to  $10^6$  times before the next particle impinges, *i. e.*, the surface is well mixed on a length scale of about 1  $\mu$ m, and internal fluctuations due to the discrete nature of the reaction processes are averaged out. With increasing pressure, however, smaller and smaller patches of the surface can be regarded

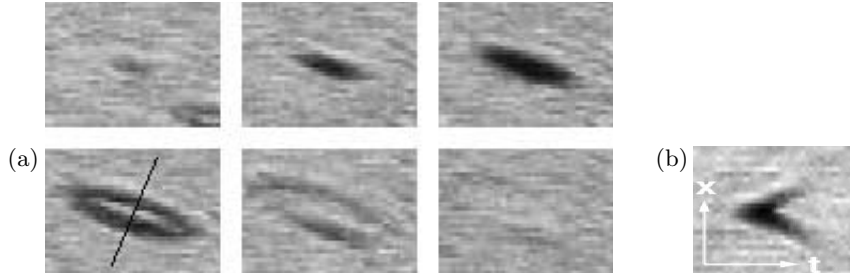


Fig. 1 – (a) Part of a Pt(110) surface exhibiting raindrop patterns recorded with EMSI (Ellipso Microscopy for Surface Imaging) [7] at  $p_{\text{CO}} = 7 \times 10^{-3}$  mbar and  $p_{\text{O}_2} = 2.2 \times 10^{-2}$  mbar. The time interval between the snapshots is 160 ms, and the depicted area is  $100 \times 70 \mu\text{m}^2$ . (b) Space-time diagram of the raindrop ( $1.6 \text{ s} \times 100 \mu\text{m}$  [8]).

as well mixed, the size of a critical nucleus that would trigger a transition wave decreases [6]. The deterministic PDE models are expected to fail and stochastic effects become relevant.

An experimental observation with Pt(110) at intermediate pressures (called “raindrop patterns”) that supports this reasoning is reproduced in fig. 1. The CO partial pressure  $p_{\text{CO}}$  had been stepwise increased to a value just before the whole surface would switch to the CO-covered state. CO nuclei could be seen to originate at various places forming a ring-shaped pattern that was subsequently destroyed (propagation failure). Their appearance seemed to be randomly distributed all over the catalyst surface [8]. In contrast, Pt(100) did not show raindrop patterns for pressures up to  $5 \times 10^{-2}$  mbar.

Thus a stochastic model is needed to complement the deterministic differential equations models. The isothermal, spatially homogeneous case was treated in [9]; the stochastic version of the model proposed there reproduces the behaviour of the mean-field equations at low pressures in the limit of large particle numbers, but it is also capable of describing stochastic effects that can be observed on sufficiently small surfaces. In order to describe the raindrop patterns properly, however, the stochastic version of the model must be extended to a nonisothermal spatial model, which will be accomplished in the sequel.

Both the deterministic and the stochastic version of our model are still based on the reconstruction model which uses the CO and oxygen coverages  $u$  and  $v$  as variables, as well as the fraction  $w$  of surface in the bulk-like ( $1 \times 1$ ) phase [9, 10]. The deterministic version corresponds, as far as the coverages and the phase variable are concerned, to the ODE model proposed in [9] to which we have added a diffusion term for CO and an equation for the surface temperature field. The equations for  $u$ ,  $v$  and  $w$  read

$$\partial_t u = k_1 p_u s_u (1 - u) - k_2(\theta, \bar{T}) u - k_3(\theta, \bar{T}) uv + D_u \Delta u, \quad (1)$$

$$\partial_t v = 2 k_4 p_v (s_v w + \tilde{s}_v (1 - w)) ((1 - u)(1 - v))^2 - k_3(\theta, \bar{T}) uv, \quad (2)$$

$$\begin{aligned} \partial_t w = k_5(\theta, \bar{T}) ((1 - \alpha) u^4 + \alpha w^4) (1 - w) - \\ - k_6(\theta, \bar{T}) ((1 - \alpha) (1 - u)^4 + \alpha (1 - w)^4) w \end{aligned} \quad (3)$$

( $p_u, p_v$ : partial pressures of CO and oxygen;  $k_1, k_4$ : impingement rates;  $k_2, k_3, k_5, k_6$ : Arrhenius rates ( $\theta, \bar{T}$  are defined below);  $s_u$ : sticking probability of CO;  $s_v, \tilde{s}_v$ : sticking probability of O on  $1 \times 1$  and  $1 \times 2$  phase;  $\alpha$ : weight parameter. All parameters as in [9] if not indicated otherwise.) In order to derive an evolution equation for the surface temperature from an energy balance, we assume that below an infinitesimal surface area  $dx_1 dx_2$  around a point  $x = (x_1, x_2)$  on the surface, the crystal has temperature  $T(x)$  in a cube of volume

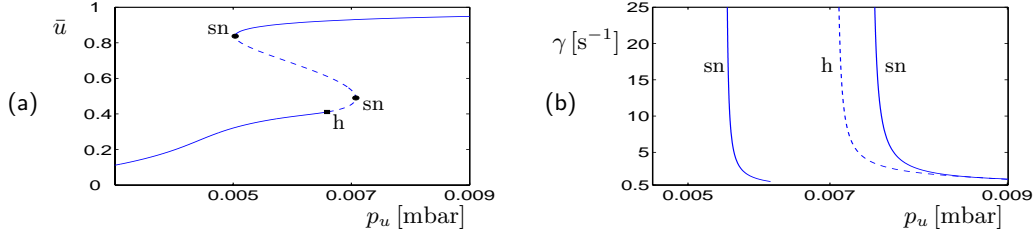


Fig. 2 – (a) Continuation of equilibrium CO coverage  $\bar{u}$  in  $p_u$  for the thermo-kinetic model,  $\gamma = 10^3 \text{ s}^{-1}$ . There is a Hopf bifurcation point (h) between two saddle-node bifurcation points (sn). (b) Continuation of Hopf and sn bifurcations in  $p_u$  and  $\gamma$ .

$l_T dx_1 dx_2$ , where  $l_T$  is a characteristic depth for the penetration of heat effects into the solid. Moreover, we assume that the bulk below the cube has temperature  $T_b[T]$ , *i.e.*, the bulk temperature is a functional of the surface temperature field. This assumption is due to the fact that the bulk temperature is regulated by a feedback mechanism according to the surface temperature in order to heat or cool the surface. The energy balance of the cube is then given by  $dU = dQ_{\text{chem}} + dQ_{\text{rad}} + dQ_{\text{cond}}$ , where  $U$  denotes internal energy, and  $dQ_{\text{chem}}$ ,  $dQ_{\text{rad}}$  and  $dQ_{\text{cond}}$  are the changes of internal energy through production and transfer of heat by chemical reactions, radiation and heat conduction, respectively. The equation for  $T$  follows from  $dU/dt = \partial T/\partial t C \rho_b l_T dx_1 dx_2$ , where  $C$  is the heat capacity and  $\rho_b$  the bulk density of platinum. Linearising the resulting equation around a reference temperature  $\bar{T}$ , for which we choose the equilibrium temperature of an empty surface, and rescaling the temperature variable to  $\theta = (T - \bar{T})/\bar{T}$  yields

$$\begin{aligned} \partial_t \theta = \beta(\bar{T}) [H_1 k_1 p_u s_u (1 - u) - H_2 k_2(\theta, \bar{T}) u + H_3 k_3(\theta, \bar{T}) uv + \\ + H_4 k_4 p_v (s_v w + \tilde{s}_v (1 - w)) ((1 - u)(1 - v))^2] - \gamma(\bar{T}) \theta + D_\theta \Delta \theta, \end{aligned} \quad (4)$$

where  $\beta(\bar{T})$  represents an inverse heat capacity, and  $\gamma(\bar{T})$  the effectivity of the feedback;  $H_1 = 135 \text{ kJ/mol}$ ,  $H_2 = H_1$ ,  $H_3 = 30 \text{ kJ/mol}$ , and  $H_4 = 230 \text{ kJ/mol}$ , are the heat of adsorption of CO, the heat loss by desorption of CO, the heat of reaction and the heat of adsorption of oxygen, respectively. (See [11] for a somewhat different temperature equation for a platinum foil.) As it turns out,  $\beta$  and  $\gamma$  are determined once  $\bar{T}$  and the characteristic depth  $l_T$  have been fixed. (For more details see [12].)

For large  $\gamma$  and not too high reaction rates the system would remain isothermal. Hence, thermal effects can be analysed using  $\gamma$  as bifurcation parameter. Thermokinetic effects are a consequence of the asymmetric inhibition of adsorption and the strong temperature dependence of CO desorption. An O-covered surface exhibits a high reaction rate and therefore becomes hot, while a high CO-coverage keeps the catalyst cool. Since, in turn, a lower temperature favors CO coverage through reduced desorption, the effect is autocatalytic.

A partial bifurcation analysis of the model is reproduced in fig. 2. For large  $\gamma$ , CO pulses propagate on the O-covered surface for relatively long times for  $p_u$  close to the Hopf bifurcation. With decreasing  $\gamma$  this bifurcation shifts to slightly higher  $p_u$ , which moves the O-covered branch away from the region of excitability such that the pulses shrink faster (see fig. 3). Physically this can be readily explained by temperature effects due to changes in the reaction rate. The rate drops sharply on predominantly CO-covered areas because oxygen adsorption is blocked there. Behind the CO pulses, however, the reconstruction has been lifted and the reaction rate increases to values even higher than on the original O-covered  $1 \times 2$  surface because of the higher sticking coefficient of oxygen on the  $1 \times 1$  phase. Consequently, the

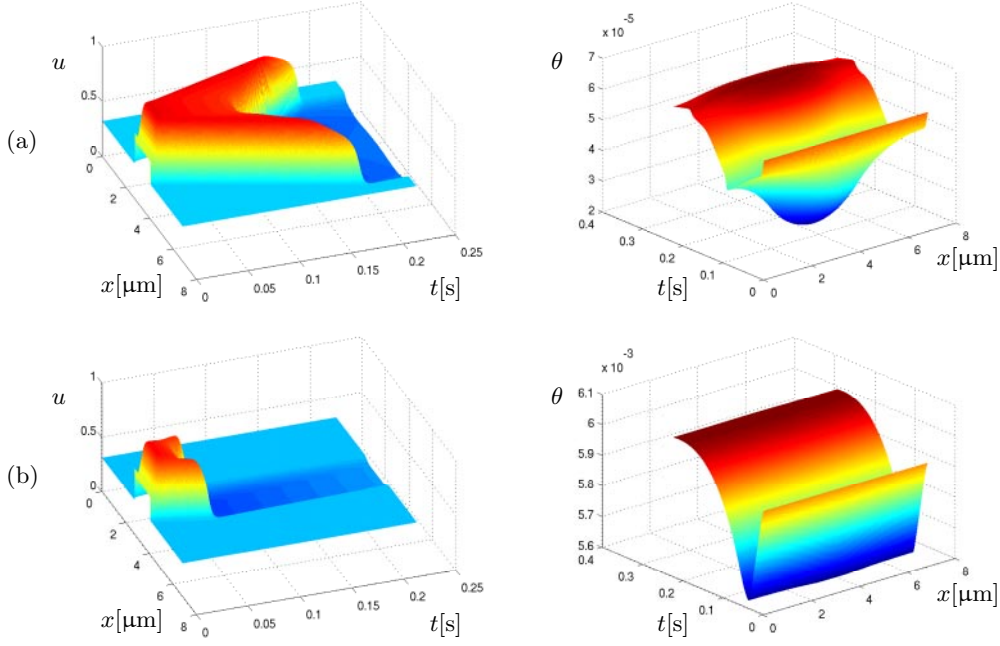


Fig. 3 – Simulation of pulse propagation using the thermo-kinetic model eqs. (1)-(3) and (4) in one space dimension with no-flux boundary conditions. A CO nucleus was put in the initial conditions on an otherwise predominantly O-covered surface. (a) For  $\gamma = 10^3 \text{ s}^{-1}$  pulses form and propagate, but finally die due to rising temperature. (b) For  $\gamma = 10 \text{ s}^{-1}$  pulses can still be formed but die quickly. The parameters are  $p_u = 5.0 \times 10^{-3} \text{ mbar}$ ,  $p_v = 1.55 \times 10^{-2} \text{ mbar}$ ,  $D_u = 10^{-12} \text{ m}^2/\text{s}$ , and  $\bar{T} = 520 \text{ K}$ . In the depicted simulations heat conduction was chosen unrealistically slow in order to visualize where heat production takes place. The effect of nucleation and propagation failure, however, persists even with realistic heat diffusion.

temperature locally rises to values even higher than at the beginning. Since heat conduction is fast, the CO pulses are overrun from the inside (because a hotter surface cannot maintain a high CO coverage due to increased desorption). In contrast, for slightly higher CO pressure ( $p_u \gtrsim 5.5 \times 10^{-3} \text{ mbar}$ ) the whole surface ends up in the CO-covered (cooler) state.

In order to model stochastic effects, the surface is divided into a square lattice of cells of mesoscopic size indexed by  $i = (i_1, i_2)$ , each containing  $n$  adsorption sites. These cells are regarded as well mixed and must therefore be chosen smaller than the diffusion length. The state of a cell is defined by the vector  $(U(i, t), V(i, t), W(i, t))$ , where  $U$ ,  $V$ , and  $W$  denote the numbers of CO molecules, oxygen atoms, and  $1 \times 1$  sites, respectively, and the (rescaled) temperature  $\theta(i, t)$ . The elementary processes are formulated as births and deaths of molecules with transition probabilities corresponding to the terms in eqs. (1)-(3). (See, *e.g.*, [13].) If the rate of a process in the deterministic model is  $K(u, v, w, \theta)$  then the probability per unit time for the corresponding transition in cell  $i$  is  $n K(U(i)/n, V(i)/n, W(i)/n, \theta(i))$ . Along with adsorption, desorption, and reaction events in a certain cell  $i$  goes an instantaneous increase (or decrease) of  $\theta(i, t)$ . The adsorption of a CO molecule in cell  $i$ , for instance, leads to an increase of  $\theta(i, t)$  by  $\frac{1}{n}\beta(\bar{T})H_1$ . Hence, the  $\theta(i, t)$  are random variables as well. Diffusion of CO is included by specifying a probability for the transition of a CO molecule to a neighboring cell, *i.e.*, for a decrease by one of  $U(i)$  in a certain cell  $i$  and a simultaneous increase by one in an adjacent cell. The temperature feedback and heat conduction result

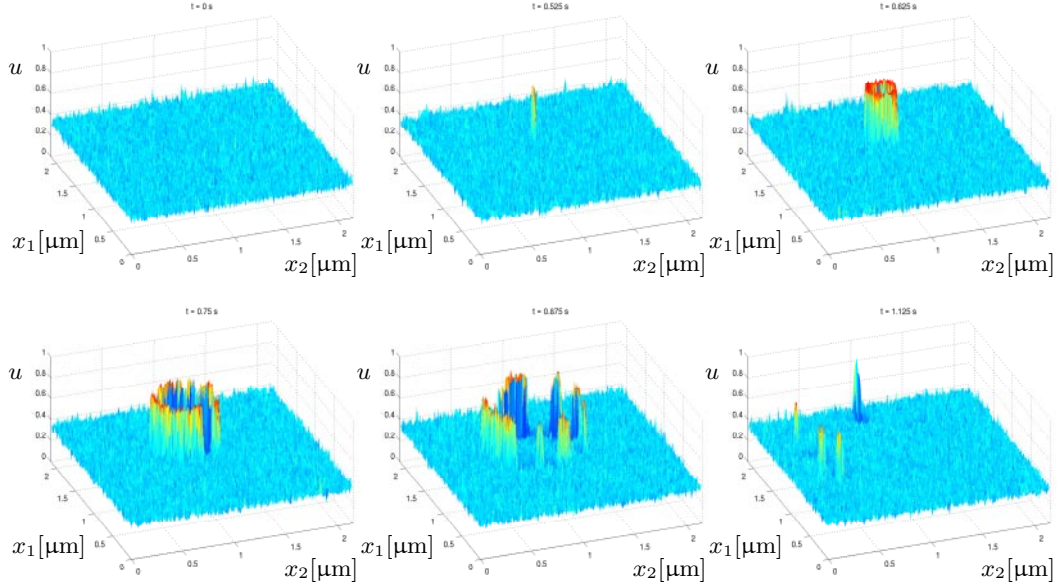


Fig. 4 – Two-dimensional stochastic simulation of raindrop patterns on a predominantly O-covered Pt(110) surface using the stochastic model with periodic boundary conditions and thermo-kinetic effects included (cf. fig. 3a). Spontaneous nucleation of a CO pulse occurs due to coverage fluctuations. The simulation was performed with  $200 \times 200$  cells,  $n = 10^3$  adsorption sites per cell, and  $p_u = 5.22 \times 10^{-3}$  mbar,  $p_v = 1.55 \times 10^{-2}$  mbar, CO diffusion corresponding to  $D_u = 1.4 \times 10^{-14}$  m<sup>2</sup>/s,  $\bar{T} = 520$  K,  $\gamma = 10^3$  s<sup>-1</sup>.

in a so-called drift (a “deterministic” change) of the  $\theta(i, t)$  that is computed according to the deterministic terms. (For heat conduction we either use a discretized Laplacian, or we work with a global temperature variable.) The stochastic process thus characterized is a (space-time) Markov jump process with inter-jump drift. For stochastic simulations we have implemented an algorithm similar to the one proposed in [14].

As long as CO diffusion is fast compared to the remaining processes, which corresponds to low-pressure conditions, stochastic simulations essentially do not differ from deterministic ones. In particular, no spontaneous nucleation in bistable or excitable regions could be observed. For parameter values that are realistic for intermediate pressures ( $n = 10^3$  sites per cell, rate of transition of CO molecules to neighboring cells corresponding to  $D_u = 1.4 \times 10^{-14}$  m<sup>2</sup>/s), however, fluctuations clearly become visible and critical nuclei do form spontaneously. A computer simulation with  $200 \times 200$  cells at  $p_v = 1.55 \times 10^{-2}$  mbar of nucleation, pulse formation and propagation failure is reproduced in fig. 4. Similar results are obtained in simulations with  $300 \times 300$  cells and  $5 \times 10^2$  sites per cell.

The homogeneous nucleation rate on an ideal surface can be estimated from an analysis of large deviations (see, *e.g.*, [15]) under the assumption that the sites in a patch of critical size  $n_{cr}$  are CO-covered independently with probability  $\bar{u}$ ,  $\bar{u}$  being the equilibrium CO coverage from the deterministic model. For a critical coverage  $u^* > \bar{u}$ , the fraction of time the patch has CO coverage  $u \geq u^*$  is assumed to be given by the probability  $P[u \geq u^*]$ . It can be derived that, for not too small  $n_{cr}$ , this probability is approximately equal to

$$\left[ \left( \frac{\bar{u}}{u^*} \right)^{u^*} \left( \frac{1 - \bar{u}}{1 - u^*} \right)^{1 - u^*} \right]^{n_{cr}}. \quad (5)$$

The value of  $u^*$  is obtained from the null-clines of the deterministic model; the value of  $n_{cr}$  decreases linearly with the pressure and lies between  $10^3$  and  $10^4$  at  $10^{-2}$  mbar [6]. We estimate the rate of events by multiplying the above expression with the density of adsorption sites and dividing by a characteristic time for which we take the time required for the impingement of one monolayer of molecules from the gas phase. The resulting function is obviously very sensitive to  $n_{cr}$  but also depends crucially on the excitation threshold  $u^* - \bar{u}$ . Reasonable values [7] of 1 to 100 events /mm<sup>2</sup> s are obtained with  $n_{cr} = 3000$ –4000,  $u^* = 0.41$  and  $0.33 < \bar{u} < 0.35$ . Increasing  $n_{cr}$  by one order of magnitude (which would correspond to a pressure decrease by one order) yields values indistinguishable from zero.

Of course, surface inhomogeneities always play a role on real catalysts. Nevertheless, the experimental observations are reproduced by a realistic stochastic model that includes temperature effects. This suggests that at least a significant fraction of the observed nuclei form homogeneously. The presented effect, *i.e.*, the raindrop patterns, therefore constitutes the first example of mesoscopic pattern formation (1–100  $\mu\text{m}$ ) in a surface reaction that is initiated by internal fluctuations and cannot be fully captured in a deterministic description.

\* \* \*

JS and CR acknowledge financial support by the *Deutsche Forschungsgemeinschaft* (SFB 359 and IGK 710).

#### REFERENCES

- [1] ERTL G., *Science*, **254** (1991) 1750.
- [2] EISWIRTH M. and ERTL G., *Chemical Waves and Patterns*, edited by KAPRAL R. and SHOWALTER K. (Kluwer, Dordrecht) 1995, p. 447.
- [3] EISWIRTH M. and ROTERMUND H. H., *Physica D*, **84** (1995) 40.
- [4] SUCHORSKI Y., BEBEN J., JAMES E. W., EVANS J. W. and IMBIHL R., *Phys. Rev. Lett.*, **82** (1999) 1907.
- [5] SUCHORSKI Y., BEBEN J., IMBIHL R., JAMES E. W., LIU D.-J. and EVANS J. W., *Phys. Rev. B*, **63** (2001) 165417.
- [6] BÄR M., ZÜLICHE M., EISWIRTH M. and ERTL G., *J. Chem. Phys.*, **96** (1992) 8595.
- [7] ROTERMUND H. H., *Surf. Sci. Rep.*, **29** (1997) 265.
- [8] ROTERMUND H. H., *Surf. Sci.*, **386** (1997) 10.
- [9] REICHERT C., STARKE J. and EISWIRTH M., *J. Chem. Phys.*, **115** (2001) 4829.
- [10] KRISCHER K., EISWIRTH M. and ERTL G., *J. Chem. Phys.*, **96** (1992) 9161.
- [11] CISTERNAS J., HOLMES P., KEVREKIDIS I. G. and LI X., *J. Chem. Phys.*, **118** (2003) 3312.
- [12] REICHERT C., PhD Thesis, to be published (Universität Heidelberg) 2006.
- [13] GARDINER C. W., *Handbook of Stochastic Methods* (Springer, Heidelberg) 1985.
- [14] GILLESPIE D. T., *J. Chem. Phys.*, **115** (2001) 1716.
- [15] DURRETT R., *Probability: Theory and Examples* (Duxbury Press, Belmont) 1996.